Practical Aspects of Partial Discharge Measurement for HVDC Cables

X Hu[1,3], A J Reid[2], E Corr[3], W H Siew[3], M D Judd[4], M Seltzer-Grant[5], R Giussani[5] and O El Mountassir[6]

[1] Guizhou University, Guiyang, China
[2] Cardiff University, The Parade, Cardiff CF24 3AA, UK
[3] University of Strathclyde, 204 George Street, Glasgow G1 1XW, UK
[4] High Frequency Diagnostics and Engineering Ltd, Glasgow G3 7JT, UK
[5] High Voltage Partial Discharge Ltd, Manchester, UK
[6] Scottish and Southern Electricity Networks, 1 Waterloo Street, Glasgow G2 6AY, UK

E-mail: xhu3@gzu.edu.cn

Received xxxxxx
Accepted for publication xxxxxx
Published xxxxxx

Abstract

High-voltage direct current (HVDC) cables are increasingly being installed to connect new offshore wind farms. Unplanned outages of these connectors can cause high economic impacts. Hence, there are requirements for condition-based maintenance that can improve operational reliability. Partial discharge (PD) is indicative of insulation defects. PD monitoring for AC cables is well established, but before applying the technique to HVDC cable connections, it is important to characterise PD behaviour under DC conditions and the attenuation in HVDC cables. This paper investigates PD activity under non-ideal DC stress, PD signal attenuation in HVDC cables, and electromagnetic noise in converter stations. Under the voltage of superimposed DC and harmonics, PD pulses tend to synchronise with the phase of harmonics. Therefore, synchronised recording of PD pulses can produce phase resolved patterns as an additional tool for insulation diagnostics. Modelling of attenuation in a HVDC transmission cable indicates that a detection bandwidth of tens of kHz to a few MHz may improve detection sensitivity when measuring PD current pulses over very long cable runs is carried out through sensors such as high frequency current transformers (HFCTs) installed at cable ends. Additionally, the RF spectrum measured in a converter station cable hall did not include any switching-related signals, demonstrating the viability of RF sensors based PD monitoring for the HV components associated with the cable connections.

Keywords: HVDC transmission, Power cables, Partial discharges, Condition monitoring

1. Introduction

Offshore wind generation is moving towards sites further from the shore (e.g., tens of km and more) to access better wind conditions and increased space [1]. Long subsea interconnections are in favour for high-voltage direct current (HVDC) transmission, but conventional HVDC transmission based on line-commutated converters (LCC-HVDC) is unsuitable for connections to offshore wind farms for reasons including the large physical size of the converter station and susceptibility to commutation failures. However, the development of commercially viable voltage-source converters (VSC) over the last decade has made possible the use of HVDC for offshore connections. VSC-HVDC

technologies also permit the use of extruded cables which, compared with mass impregnated cables, are typically cheaper, easier to install and maintain, and can operate with higher conductor temperatures [2]. However, there is relatively little field experience concerning how extruded cables age electrically under HVDC voltage stress and limited data regarding their long-term reliability. Therefore, a range of studies aimed at investigating the reliability of extruded HVDC cables are being carried out [3]-[5]. Some of these studies are particularly focused on space charge formation and measurement [6], [7] while others are investigating PD in extruded HVDC cable systems [8], [9].

Partial discharge (PD) is a well-known indicator of insulation ageing and degradation under AC conditions. On-line PD monitoring of AC power equipment has been employed by operators in the context of condition-based and predictive maintenance [10]. Under pure DC conditions, PD has received less attention because it is less directly associated with causing insulation degradation and breakdown [11]. However, as the number of DC applications in power systems continues to grow, along with maintenance trends moving in the direction of predictive maintenance, PD monitoring of insulation under DC stress is becoming increasingly important. Early research into PD in HVDC cables was mostly concerned with mass impregnated types [12], [13]. A thorough review of PD at DC voltage was carried out by Morshuis et al. [11] in 2005. Only recently have there been some discussions of PD measurement on extruded HVDC cables [9], [14]-[16]. However, not much has been reported concerning the goal of realising on-line PD monitoring of HVDC cables, investigating effects that can be present in practical situations such as actual stress conditions, very long cables (kilometres and longer), noise environment in field, and so on.

This research aims to provide a basis for implementing on-line PD monitoring of extruded HVDC cables. To this end, PD behaviour under both pure DC stress and DC with superimposed AC ripple was investigated [17]-[19]. An on-line PD monitoring system has been developed, with preliminary testing conducted in both laboratory and field environments [16]. In this paper, the findings from these earlier results [16-19] are revisited with more details of the measurement and new interpretation of the measurement results. Moreover, practical aspects of PD monitoring for HVDC cables and accessories (joints and terminations) are evaluated, including a first-ever report of characterising the attenuation in a HVDC transmission cable based on which the possibility of using sensors installed at cable ends to monitor PD over very long cable runs (such as 10 km or longer) is assessed. Furthermore, to confirm potentials of deploying RF sensors based PD monitoring for cable accessories in converter stations, on-site measurements of electromagnetic noise and interference were performed. This paper is organised as follows. The basic mechanism of PD under DC conditions is firstly discussed. Since practical DC conditions can contain harmonics, the findings of PD testing at constant DC voltage as well as DC voltage superimposed with harmonics are summarised in Sections 3 and 4. PD current pulses are attenuated quickly with propagated distance in the cables, making it difficult to monitor PD over long cable runs. Therefore, attenuation of PD signals in HVDC cables is evaluated in Section 5. Apart from PD currents, PD radiates electromagnetic waves which can be detected using RF sensors. The potential of this technique for applications in converter stations is assessed in Section 6. Finally, some initial results from PD monitoring of HVDC cables are reported.

2. PD Phenomena in HVDC Cables

To model PD under DC conditions, a common approach has been adding a parallel resistor to each of the capacitors in the 3-capacitor equivalent circuit of PD in a cavity [20], as shown in Figure 1. This modified circuit is useful because it reflects voltage division within the insulation under constant DC stress and explains the time lapse between consecutive PD pulses. After a DC voltage is applied, PD can occur once the applied voltage rises above the cavity inception voltage. Thereafter, recharging of the discharged cavity capacitance C_c occurs relatively slowly with a time constant R_bC_c via the highly resistive insulation material. This time constant (commonly referred to as recovery time) can be seconds, minutes or hours [20]. Consequently, the number of PD pulses under DC conditions is typically several orders lower than that under AC. However, in practice, DC stresses in both LCC-HVDC and VSC-HVDC systems contain harmonics (voltage ripple) that can cause a marked increase in the frequency of PD pulses in comparison with pure DC excitation [3]. Increased PD repetition rate is symptomatic of faster insulation degradation, which is more likely in the case of extruded insulation because it is less resistant to PD than mass-impregnated types [21].

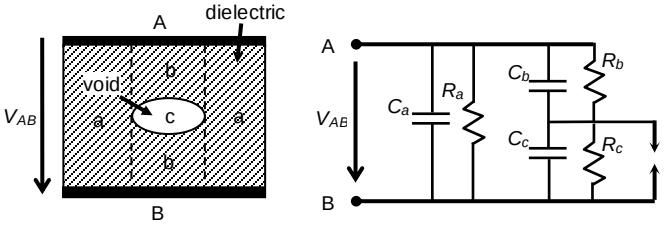

Figure 1. Modified 3-capacitor lumped-parameter equivalent circuit model [20] for DC PD in a cavity where A and B represent conductors of the HV system, a represents undamaged insulation while b represents the region of insulation affected by the presence of cavity c. V_{AB} is the DC voltage of the system, the capacitances C and resistances R have values that represent the respective insulation regions a, b and c.

PD phenomena in HVDC cables are complicated by the influences of temperature variations and by space charge that can accumulate in the bulk insulation. Temperature variations can be caused by different operational and environmental conditions. Insulation resistance usually decreases significantly with increasing temperature, reducing the recovery time so that PD occurs more frequently. Space charge (which is easily trapped in extruded insulation) distorts the electric field, causing increased electric stress that makes PD more likely to occur.

3. Measurement of PD in XLPE Cables under DC Excitation

Defective cable joint samples were fabricated using cross-linked polyethylene (XLPE) insulated cables rated at 33 kV AC. Before jointing, an artificial defect was created in the outer semi-conductive screen or the insulation of a cable section. This cable section with the defect was then jointed with another cable section without any defect to form a sample as shown in Figure 2.

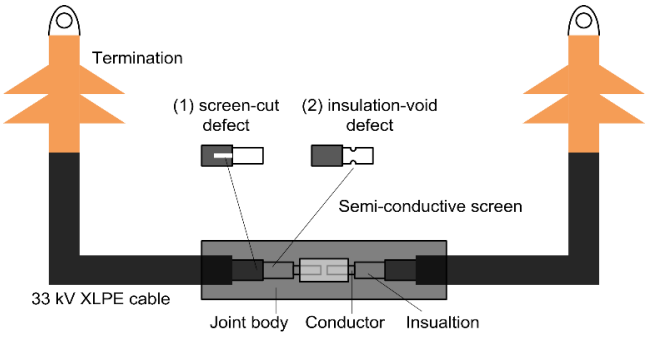

Figure 2. Test samples of cable joint containing artificial defects. (1) Screen-cut defect was a scratch on the cable semi-conductive screen. (2) Insulation-void defect was created by cutting a circular groove around the outer part of the cable insulation. Each sample contained only one type of defect.

Five samples including a defect-free sample were tested using an IEC-60270 PD measurement system. Figures 3 and 4 show the measurement circuits for testing under AC and DC, respectively. All the testing was carried out in a screened laboratory and the measurement setup (without connecting any sample) was confirmed PD-free at the rated highest voltage. Following the procedures specified in IEC-60270, the measurement setup was calibrated via injecting 500 pC through the terminals of the sample under test. The detection threshold was about 15 pC in case of the 500 pC calibration. This threshold however changes dynamically with the attenuator setting of the measurement system. The attenuator setting was manually adjusted during the measurement to accommodate the largest PDs.

Testing under AC excitation was conducted in the first place to confirm that the defects were created appropriately a-

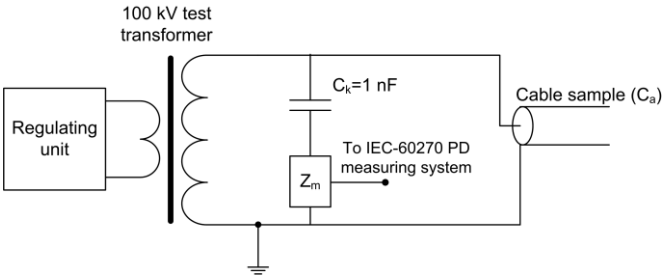

Figure 3. Measurement circuit for PD testing at AC voltages. C_k is a coupling capacitor. Z_m is an IEC-60270 compliant PD measuring impedance. The IEC PD measuring system is LDS-6.

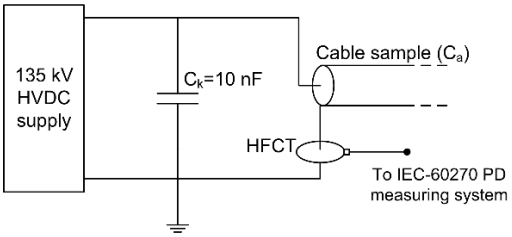

Figure 4. Measurement circuit for PD testing at DC voltages. A high frequency current transformer (HFCT) with transfer impedance 4.3 V/A and bandwidth 100 kHz – 20 MHz is used for measuring PD in this setup.

nd establish a baseline for the PD inception voltage. The testing showed that for a screen-cut sample and two insulation-void samples the PD inception voltage was around 19 kV rms while it was 35 kV rms for the other screen-cut sample and 40 kV rms for the defect-free sample. Testing under DC excitation was carried out through increasing the applied voltage stepwise by 10 kV and at each voltage level waiting for 2 minutes to confirm if PD can occur repetitively before proceeding to the next voltage level. If repetitive PD was observed, the voltage was held (no longer increased) and PD was recorded for maximum 10 hours depending on the PD activity during the test. After the recording was finished, the voltage was decreased. To excite PD in as many samples as possible, the applied voltage was up to 80 kV DC (4 times the rated phase-to-earth voltage of the cable which is 33 kV/$\sqrt{3}$ = 19 kV). Summary findings are that PD pulses are more likely to occur around the voltage ramping intervals, whereas under steady-state DC, repetitive PD was only observed in two samples (an insulation-void sample and a screen-cut sample). Figure 5 shows the 10-hour testing results for the sample containing an insulation-void defect. In total, 35,752 PD pulses were measured over the test duration of 36,331 s, an average repetition rate of about 1 pulse/s. Note that the largest pulses (reaching 1,300 pC) had their magnitude clipped by the selected measurement range of the measuring system. However, this was an acceptable compromise in order to maintain the required detection sensitivity to capture the majority of low-level pulses. Two extra 10-hour tests at 70 kV DC were carried out for this sample during which the PD activity became more vigorous, with a few pulses reaching

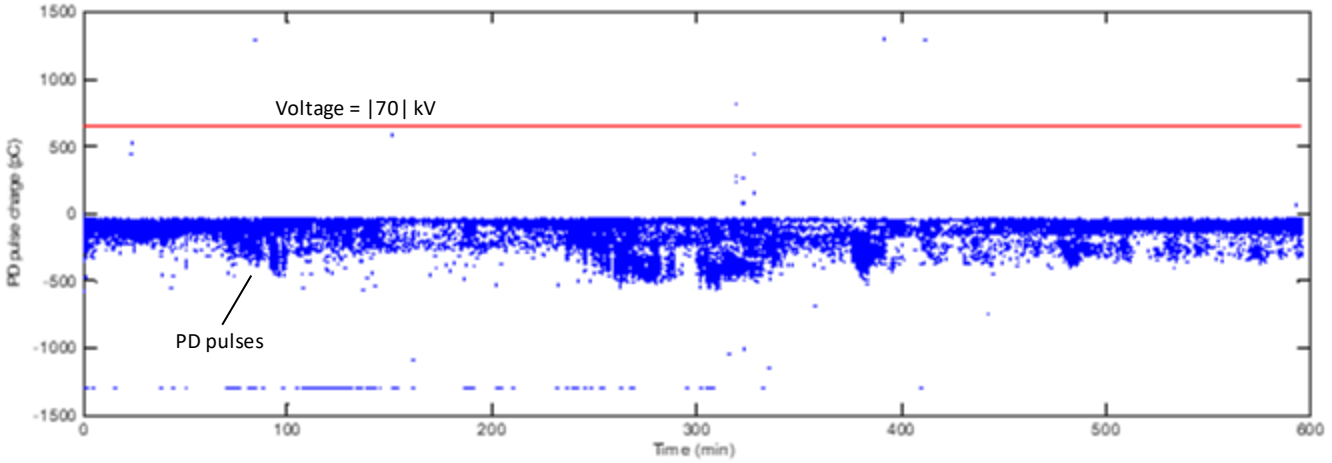

Figure 5. PD measurements over a 10-hour soak test of the cable sample with an insulation-void defect. Subject to the measurement setup under DC, the polarity of the PD pulses was supposed to be negative. Those sporadic positive pulses were considered as a result of space charge stored locally in the insulation and influencing the local electric field.

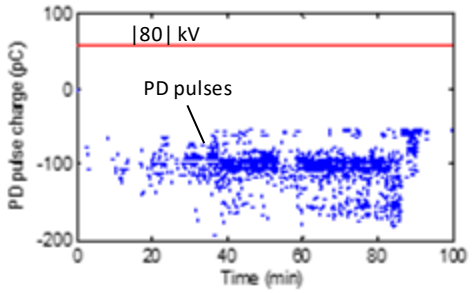

Figure 6. PD testing of the cable sample with a screen-cut defect. This was the first 100 minutes of a 5-hour test. No further PD occurred between 100 and 300 minutes.

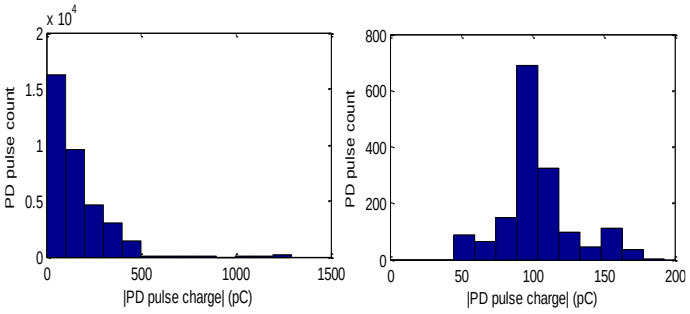

Figure 7. Histograms of the PD testing results. (a) insulation-void, (b) screen-cut.

8,000 pC. Figure 6 shows that for the screen-cut defect sample, PD reoccurred for almost 100 minutes with the highest PD magnitude close to 200 pC and an average repetition rate of 0.27 pulse/s. The PD behaviour effectively stopped after 92 minutes for this sample.

Histograms counting PD pulses whose charge falls in a defined set of ranges are one of the methods to analyse PD testing results under DC, which is recommended in a 2015 amendment to IEC-60270 [22]. Figure 7 shows histograms of the previous DC PD measurements. Interestingly, the histogram of the screen-cut defect is distributed around a central peak, whereas that of the insulation-void shows decreasing number of PD pulses at larger PD magnitudes.

4. Measurement of PD in Solid Dielectrics under Superimposed DC and AC Excitation

Switching harmonics are an inevitable occurrence in HVDC systems. In an ideal 6-pulse LCC-HVDC converter, harmonics of the power frequency present in the DC voltage are $6^{th}, 12^{th}, \ldots, 6*n$ (n = 1, 2, 3…). Under no-load conditions, the relative magnitude of the first four harmonics is listed in Table 1 [23]. In a VSC-HVDC system with PWM, the current flowing into the DC side contains harmonics that cause voltage ripple including the 3^{rd} order harmonic and higher-order harmonics around the switching frequency of IGBT devices in the converter. Their magnitude depends on the DC side capacitor size and on the switching frequency [2].

Table 1. Idealised DC voltage harmonics of a 6-pulse converter.

Harmonics	Harmonic frequency	Amplitude (rms) relative to DC
6^{th}	300 Hz	4.04 %
12^{th}	600 Hz	0.99 %
18^{th}	900 Hz	0.44 %
24^{th}	1200 Hz	0.25 %

To investigate effects of voltage ripple on DC PD behaviour, testing of three samples representing corona discharge, internal discharge and surface discharge respectively was carried out with the setup shown in Figure 8 [17]. A programmable signal generator was used to define the DC plus ripple waveform and this low voltage was amplified using an HV power amplifier for application to the test

objects. The applied voltage was monitored via a built-in 3,000:1 voltage divider of the HV amplifier and synchronised with PD measurement using an HFCT to give phase-resolved PD (PRPD) patterns.

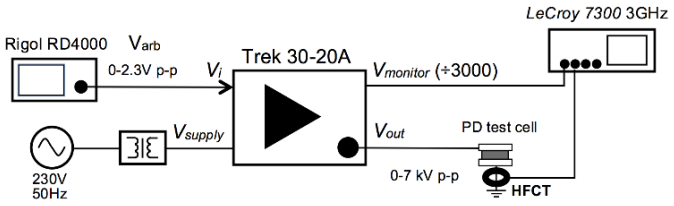

Figure 8. Experimental setup for studying effects of voltage ripple on DC PD characteristics. PD pulses were measured using an HFCT (transfer impedance 4.3 V/A, bandwidth 100 kHz – 20 MHz) clamped around the earth lead from the test object.

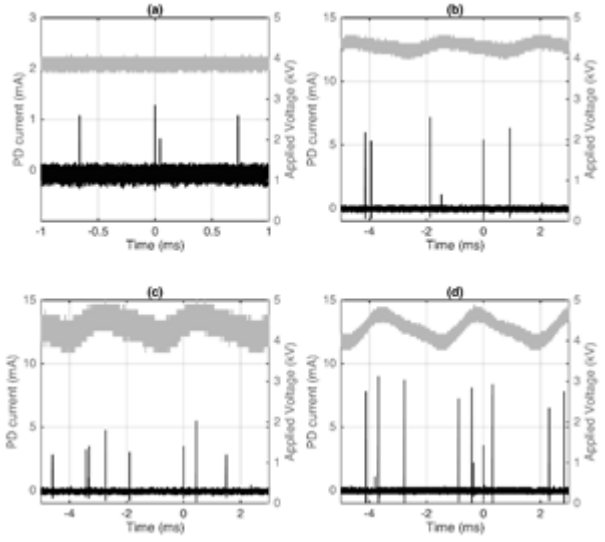

Figure 9. Effect of harmonic amplitude on PD repetition for a corona discharge source [17]. (a) DC only, (b) 5% 6th harmonic, (c) 10% 6th harmonic, (d) 15% 6th harmonic.

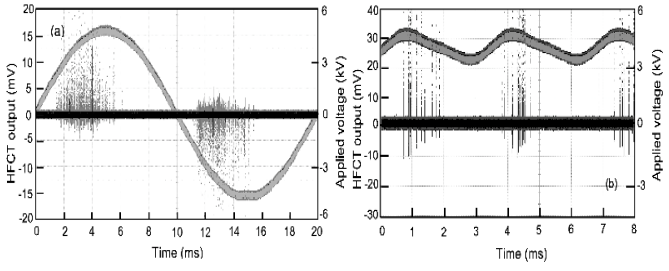

Figure 10. Internal discharge sample [17]. (a) AC PRPD pattern, (b) Superimposed DC and 30% 6th harmonic PRPD pattern synchronised with the 6th harmonic period.

Figure 9 shows examples of PD activity recorded at different levels of the 6th harmonic. Unsurprisingly, these results indicate that as the harmonic amplitude increases, PD pulses are increasingly correlated with the phase of the harmonic. While PD also occurred under pure DC voltage, its amplitude was much lower than when the harmonic was present. To compare with PD under purely AC, PRPD patterns from both applications of AC voltage and DC voltage with ripples were plotted [17]. It is observed that under AC voltage PD behaviour is as expected in that PD may occur at voltage peaks of either polarity, or on the rising or falling slopes of the power frequency cycle, depending on the type of insulation defect. In case of DC voltage with ripples, for all the three samples PD seems to predominantly cluster around the ripple peaks. For example, the results for the internal discharge sample are shown in Figure 10 where PD under AC is mostly concentrated in the 1st and 3rd quadrants of the power cycle, but under DC with ripples PD tends to occur at the ripple peaks and on the falling slopes thereafter.

5. Evaluation of High Frequency Attenuation in HVDC Cables

The PD measurement in the previous section was carried out according to IEC-60270. The measurement technique is often considered as the conventional method and has limited applications in field testing since at industrial sites there can be very high electromagnetic noise and interference in the measurement band (e.g., 100 – 500 kHz) of this method. Therefore, field testing typically acquires PD signals at higher frequencies (e.g., > 1 MHz) to avoid the background noise, and these methods are termed non-conventional methods [24]. For power cables, a widely practiced non-conventional method is based on installing HFCTs (e.g., transfer impedance 5 V/A, bandwidth 100 kHz – 10 MHz) at cable ends to monitor PD in the cables and accessories [24]. Since PD can occur in cable sections which are hundreds of metres even thousands of metres from cable ends, it will be of interest to predict, for varied cable lengths, the sufficient PD level that will allow the detection of the PD at the cable far end.

5.1 Measurement of Attenuation in HVDC Cables

PD pulses propagating in power cables are subject to attenuation that increases with frequency, reducing both the magnitude and -3 dB bandwidth of the PD pulses. For cables with extruded insulation, the attenuation is primarily due to the semi-conductive layers (made of lossy and dispersive materials) that form the interfaces between cable conductors and insulation. The frequency-dependent attenuation of the PD pulses can be approximated linearly as $\alpha_1\omega$ where α_1 is a constant in Nepers–s/m and ω is radial frequency. Some distribution cables (XLPE insulated) were reported to have α_1 in the range of 2.44e-11 to 6.72e-11 Nepers–s/m [25]. There have been fewer reports on the attenuation of transmission class cables. While α_1 equal to 4.78e-11 and 9.71e-11 Nepers–s/m was reported in [26], none has been found for HVDC transmission cables. In this work, the propagation constant $\gamma(\omega)$ of a 200 kV HVDC XLPE cable was measured using the

calibrated time-domain reflection method [27]. The method requires two pulse reflection measurements: one short-circuit measurement without attaching the sample and the other one with the sample attached and open-circuited at end. The propagation constant of the sample under test can be derived using

$$e^{-\gamma(\omega)\cdot 2l} = \frac{\mathrm{FFT}(V_{sample})\times\mathrm{FFT}(V_{sc})}{[\mathrm{FFT}(V_{adapter})]^2-[\mathrm{FFT}(V_{sc})]^2} \quad (1)$$

where l is the length of the sample, V_{sc} is the reflected pulse in the short-circuit measurement, and V_{sample} and $V_{adapter}$ are the reflected pulses in the other measurement where V_{sample} is reflected from the end of the sample and $V_{adapter}$ is reflected from the connection adapter between the measurement setup and the sample. The real part of the measured propagation constant, i.e., the cable attenuation $\alpha(\omega)$ and a linear approximation to the attenuation with $\alpha_1\omega$ (α_1 = 7.82e-11 Nepers–s/m), is shown in Figure 11. Therefore, α_1 of the 200 kV HVDC cable was in the same order as that reported earlier for distribution and transmission class XLPE cables.

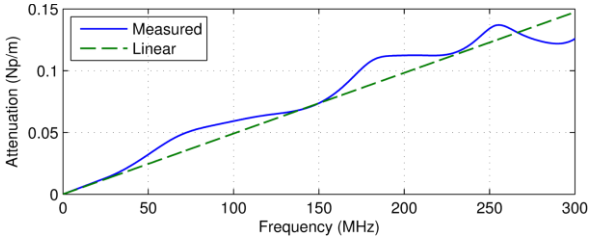

Figure 11. Attenuation of a 200 kV HVDC XLPE cable as a function of frequency.

5.2 Measurement of Attenuation in HVDC Cables

Signal attenuation resulting from propagating in the cable can be evaluated using

$$\mathrm{FFT}(V_2) = \mathrm{FFT}(V_1)\cdot e^{-\gamma(\omega)\cdot(L_2-L_1)} \quad (2)$$

where V_2 and V_1 are the signals at the propagated distance L_2 and L_1 respectively. Assuming V_1 is an original pulse measured very close to a PD source, i.e., $L_1 \approx 0$ m, the attenuated pulse after propagating L m in the cable can be obtained as

$$V_L = \mathrm{IFFT}[\mathrm{FFT}(V_1)\cdot e^{-\gamma(\omega)\cdot L}] \quad (3)$$

Considering a Gaussian pulse with a 1 ns rise time and a -3 dB bandwidth of 200 MHz at $L_1 = 0$ and using (2), Figure 12 shows the reduction in pulse bandwidth with propagated distance over the range L = 10 – 100,000 m. These calculations indicate that propagating for 1,000 m in the cable can reduce the -3 dB bandwidth of the Gaussian pulse to less than 1 MHz, while after 10,000 m the bandwidth may be reduced to less than 0.1 MHz.

For investigating attenuation of PD pulse magnitude in the cable, original pulses with the various shapes and bandwidths listed in Table 2 were considered. This is to account for the fact that PD pulse characteristics can vary over a wide range, e.g., original PD pulses as short as few ns and those with a time duration of tens of ns can be observed [28]. Attenuation of the pulse magnitude was evaluated from a practical PD detection perspective, i.e., assuming a measurement system with a detection threshold of 5 mV (pulse magnitude), the minimum detectable pulse magnitude $PM_{\mathrm{detectable}}$ into the cable can be calculated through (3) and

$$\frac{\max(V_1)}{PM_{\mathrm{detectable}}} = \frac{\max(V_L)}{5\ \mathrm{mV}} \quad (4)$$

where max(·) represents the peak absolute value of a pulse. With the linear attenuation shown in Figure 11, $PM_{\mathrm{detectable}}$ was obtained for cable lengths ranging from 100 – 100,000 m and the results are presented in Figure 13.

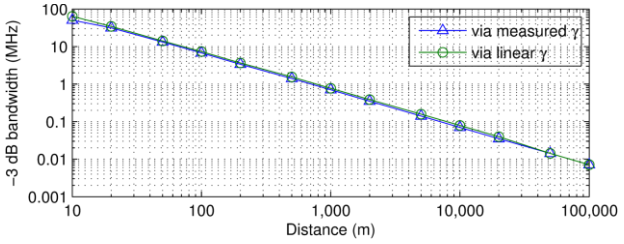

Figure 12. -3 dB bandwidth of the Gaussian pulse against the propagated distance.

Table 2. Simulated PD pulses for evaluating attenuation in the cable. These are tabulated in order of descending spectral bandwidth in accordance with the legend used in Figure 13.

Pulse shape [29]	Rise time (ns)	Pulse width (ns)	-3 dB bandwidth (MHz)
Gaussian	1.1	1.6	200
Gaussian	2.1	3	101
Wanninger	1.1	4.8	51
Double exponential	1.1	9.5	20
Double exponential	2	19	10
Wanninger	11	48	5
Double exponential	10	94	2
Double exponential	20	188	1

Taking the point associated with the two dashed lines in Figure 13 as an example, at 5,000 m from the detection position, the original pulse (10 MHz bandwidth) needs to have a minimum magnitude about 0.3 V in order to be detected. In other words, the original pulse of the 10 MHz bandwidth will attenuate from 0.3 V to 5 mV in magnitude after propagating 5,000 m in the cable. For distances over 10,000 m, Figure 13 suggests a tendency of doubled minimum detectable magnitudes when the bandwidth of the original pulse is doubled, e.g., to allow detection after 10,000 m the original pulse with the 10 MHz bandwidth should have a minimum magnitude of 0.5 V. This is doubled to 1.0 V for the original pulse with the 20 MHz bandwidth. Previous studies on measuring original PD pulses suggested that PD signals from discharges within dielectrics typically have magnitudes < 1 V [28], [29]. Based on Figure 13, it therefore seems unlikely that

pulses with bandwidth > 20 MHz will be detectable beyond 10,000 m while detection should be possible for pulses with bandwidth < 10 MHz. However, it is clear that the feasibility of detecting PD into tens of km cables will be strongly influenced by the specific high frequency attenuation of each cable type.

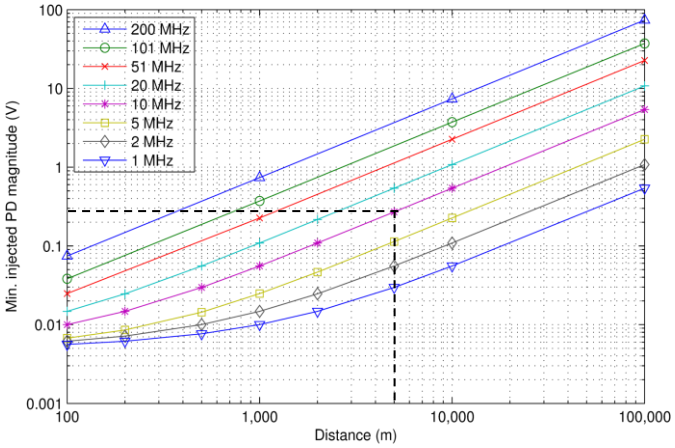

Figure 13. Minimum detectable pulse magnitude at the point of injection into the cable, assuming a detection threshold of 5 mV. The legend is labelled with -3 dB bandwidth of the original pulse as indicated in Table 2.

6. Radiated Electromagnetic Signals in HVDC Converter Stations

The infrequent nature of PD occurrence under DC means that noise and interference mitigation measures are especially important for realising effective PD detection. An IEEE Technical Committee is currently working on determining recommended practice for very high frequency (VHF)/ultra high frequency (UHF) PD measurement on HVDC cable accessories [30] and in this context it is useful to evaluate general signal characteristics in the VHF/UHF range within HVDC converter stations. Therefore, surveys of the electromagnetic environment were carried out at a converter station feeding a subsea DC transmission link cable that operates at 250 kV. There are two halls associated with each pole of the transmission link. One is the valve hall (where the switching takes place) and the other is the cable hall, which contains the filter and cable termination.

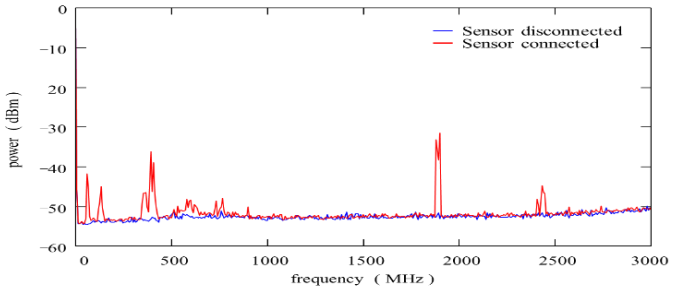

Figure 14. RF spectrum measured at the valve hall window.

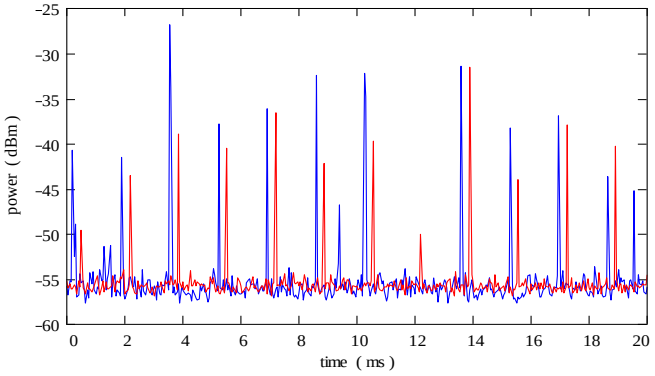

Figure 15. Synchronised point-on-wave over a power frequency cycle measured at 132.5 MHz with an RF bandwidth of 5 MHz. The red and blue traces show measurements from two different dates. The slight time/phase offset between the two readings is attributed to the line-triggering accuracy of the spectrum analyser sweep.

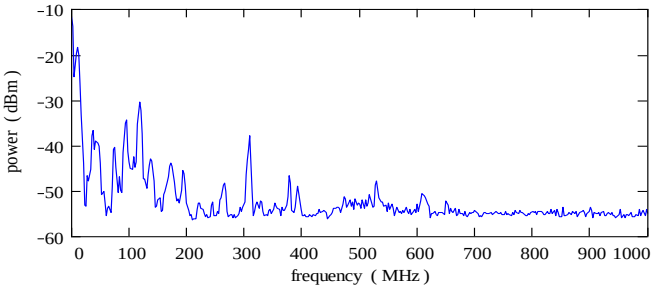

Figure 16. RF spectrum measured in the cable hall near the cable termination.

Figure 14 shows electromagnetic emissions in the VHF and UHF bands measured using an RF sensor installed on a glass window of the valve hall (entry to the hall is forbidden during operation). The peaks below 200 MHz in the frequency range were caused by switching operations of the converter. This can be illustrated by the point-on-wave RF pulses corresponding to 12 switching operations per 20 ms recorded using a spectrum analyser in zero-span mode at 132.5 MHz. Figure 15 shows the measured point-on-wave pulses recorded during two visits to the site on different dates. There are some variations in the amplitudes of the pulse peaks, which are expected to be load-dependent.

Electromagnetic emissions in the cable hall were measured with an RF sensor installed near the cable termination. Figure 16 shows the power spectrum recorded up to 1,000 MHz. For each main peak in the spectrum, the point-on-wave measurement was performed to check if they were associated with switching or the power cycle. This evaluation confirmed that these peaks were all communications-type signals. There is no evidence of any RF switching-related or electrical discharge-type signals in the cable hall which might interfere with the operation of a radiometric PD monitoring system.

7. HVDC Cable PD Monitoring

A newly developed PD monitoring system was applied to a 200 kV HVDC cable loop which was undergoing a sequence of prequalification tests as per CIGRE TB 496 [31] at a cable aging laboratory [16]. The cable loop consisted of XLPE insulated cables, two joints and two terminations. HFCTs were installed around the earth lead both at the cable joints and terminations. HFCT 1 has transfer impedance of 3.9 V/A and -3 dB bandwidth of 100 kHz – 20 MHz. HFCT 2 has transfer impedance of 1.8 V/A and -3 dB bandwidth of 350 kHz – 35 MHz. The PD monitoring system was used to record data from all the sensors simultaneously with a 100 MS/s sampling rate and a 14-bit amplitude resolution. A schematic of the experimental setup is shown in Figure 17. It should be mentioned that at the same time of PD monitoring, space charge measurement using the pulsed electroacoustic (PEA) technique was carried out on the cable loop for a separate project [32].

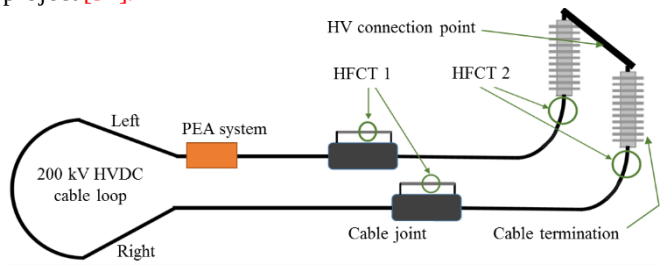

Figure 17. PD monitoring of a 200 kV HVDC cable loop.

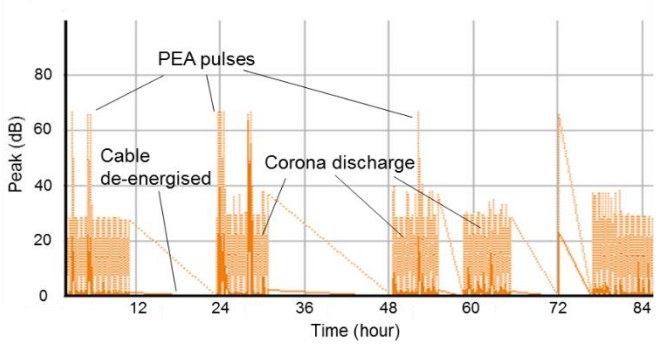

Figure 18. PD monitoring records showing peak magnitude of the pulses from the PEA system and corona discharge. The peak magnitude is plotted in dB because the PEA pulses had significantly larger magnitude than that of corona discharge. The dB level is evaluated as $20\log(V_p)$ where V_p is the peak voltage in mV.

Continuous PD monitoring was carried out for the cable loop when the applied voltage was cycling between 0 and +290 kV ($1.45*U_0$). An example of the recorded data is shown in Figure 18. The record was obtained from HFCT 1 installed at the cable joint on the right of the cable loop. Those largest signals with the peak magnitude around 67 dB were due to the HV PEA pulses injected (7 kV) during the PEA measurement. Corona discharge with the peak magnitude around 27 dB was also detected from sharp edges of the HV connection.

8. Discussion

PD testing of four defective cable samples were performed under AC and DC excitation, respectively. The results suggested that the cable samples with similar defects as well as PD inception voltages under AC may not show active PD even at DC voltages several times as high as the rated cable phase-to-earth AC rms voltage. The most active DC PD observed in a cable sample was 1 pulse/s on average over a test duration of 10 hours. Histograms of PD pulse count against PD magnitude can be an effective DC PD fingerprint in addition to basic DC PD parameters of PD magnitude and time interval between two consecutive pulses. PD testing of the corona discharge sample under DC with superimposed harmonics showed that PD tended to synchronise with the phase of the superimposed harmonic, and PD magnitude increased significantly compared with that at a purely DC voltage. While the PRPD patterns under pure AC were dependent on PD type, the PRPD patterns under DC plus harmonics had a characteristic of clustering around the voltage peaks regardless of PD types.

High frequency attenuation in a 200 kV HVDC XLPE cable was characterised as being in the same order as that reported for some AC XLPE cables. Modelling based on the measured attenuation suggested that after propagating for 10 km in the cable, the -3 dB bandwidth of PD pulses can decrease from 200 MHz to less than 0.1 MHz. Considering PD-measurement systems based on sensors such as HFCTs installed at cable ends and with a detection threshold of 5 mV, the theoretical maximum distance into which most of PD pulses with a 20 MHz initial bandwidth (equivalent to 10 ns width at half maximum) can be detected is in the region of 10 km. Increased chance of detecting after 10 km of the cable may be achieved through using sensors with a lower frequency limit of the sensor bandwidth not higher than 0.1 MHz. Furthermore, an upper limit between 1 – 3 MHz should be sufficient because PD pulse bandwidths will decrease to less than 1 MHz after 1 km.

Measurement of radiated signals in a converter station showed that in the valve hall, switching-related pulses can be observed corresponding to 12 switching operations of the converter per power frequency cycle. No switching-related pulses were found in the cable hall where the cable termination is located. However, since this measurement was carried out using an RF sensor, the observed noise spectrum was mainly in the VHF and UHF bands. Other measurements with a coupling capacitor sensor (with a lower -3 dB frequency of 5 MHz) installed at the cable termination in the same converter station did show 12 switching-related pulses per power frequency cycle [16]. The reason that these switching pulses were not observed in the higher frequency RF spectrum is because the VHF and UHF signals of the switching pulses are heavily attenuated while transmitting from the converter hall

to the cable hall and because the RF sensor had very low sensitivity at frequencies below the VHF band.

9. Conclusions

A range of topics concerning PD measurement for HVDC cables are investigated in this paper. The findings can contribute to the realm of monitoring PD for HVDC cable connections, and some conclusions are drawn as follows.

The observations concerning PD under DC voltage with ripples shed light on the correlation between the PD activity and the phase of harmonics superimposed on the DC voltage. The results also suggest that modulation of the HVDC with a modest amount of AC might help to reveal insulation defects by causing PD, which could be an effective PD measuring approach under DC.

The attenuation simulations are expected to be a useful reference in determining appropriate bandwidths for HFCT-based PD measurement systems to increase the possibility of measuring PD occurring at remote locations within very long cable runs, such as those used for connecting offshore wind farms.

Switching-related pulses can be detected using an RF sensor in the valve hall of the converter station, which may have prospect of applications to condition monitoring of the converters. The measured RF spectrum in the cable hall of the converter station seems promising for potential radiometric PD monitoring of the HV components associated with the cable connections.

Future work could involve PD testing of defective cable samples under superimposed DC and harmonics to further investigate the relationship between PD behaviour and DC voltage ripples. Additionally, studies on the relationship between switching pulse signals and the operating conditions of HVDC converters would be interesting and might lead to a new monitoring concepts for the operation of the converters.

References

[1] Bresesti P, Kling W L, Hendriks R L and Vailati R 2007 HVDC connection of offshore wind farms to the transmission system *IEEE Trans. Energy Convers.* **22** 37–43

[2] Hertem D V, Gomis-Bellmunt O and Liang J 2016 *HVDC Grids: For Offshore and Supergrid of the Future* (New Jersey: John Wiley & Sons)

[3] Morshuis P, Cavallini A, Fabiani D, Montanari G C and Azcarraga C 2015 Stress conditions in HVDC equipment and routes to in service failure *IEEE Trans. Dielectr. Elect. Insul.* **22** 81-91

[4] Mazzanti G and Marzinotto M 2017 Advanced electro-thermal life and reliability model for high voltage cable systems including accessories *IEEE Elect. Insul. Mag.* **33** 17-25

[5] Wang W 2018 The effect of ripple on the reliability of VSC-HVDC extruded cable systems *12th Int. Conf. Properties Appl. Dielectr. Mater. (ICPADM)* Xi'an 412-418

[6] Mazzanti G 2017 Space charge measurements in high voltage DC extruded cables in IEEE Standard 1732 *IEEE Elect. Insul. Mag.* **33** 9-15

[7] Wang X, Chen C, Cheng C, Wu Y, Wu K, Fu M, Hou S and Hui B 2018 Space charge characteristics in 160 kV DC XLPE cable under temperature gradient *IEEE Trans. Dielectr. Elect. Insul.* **25** 2366-2374

[8] Fard M A, Farrag M E, McMeekin S G and Reid A J 2017 Partial discharge behavior under operational and anomalous conditions in HVDC systems *IEEE Trans. Dielectr. Elect. Insul.* **24** 1494-1502

[9] Gu X, He S, Xu Y, Yan Y, Hou S and Fu M 2018 Partial discharge detection on 320 kV VSC-HVDC XLPE cable with artificial defects under DC voltage *IEEE Trans. Dielectr. Elect. Insul.* **25** 939-946

[10] Renforth L A, Hamer P S, Clark D, Goodfellow S and Tower R 2015 Continuous Remote Online Partial Discharge Monitoring of HV Ex/ATEX Motors in the Oil and Gas Industry *IEEE Trans. Ind. Appl.* **51** 1326-1332

[11] Morshuis P H F and Smit J J 2005 Partial discharges at DC voltage: their mechanism, detection and analysis *IEEE Trans. Dielectr. Elect. Insul.* **12** 328-340

[12] Morshuis P and Beyer J 1997 Quality assessment of HVDC components by PD analysis *IEEE Annu. Rep. Conf. Elect. Insul. Dielectr. Phenom.* Minneapolis 542-545

[13] Jeroense M J P, Bergkvist M and Nordberg P 1999 Partial discharges in high voltage direct current mass-impregnated cables *11th Int. Symp. HV Eng.* London 53-57

[14] Takahashi T, Wibowo A S, Cavallini A, Montanari G C, Boyer L, Luton M and Mirebeau P 2016 AC and DC partial discharge measurements on defective cables *IEEE Elect. Insul. Conf. (EIC)* Montreal 375-378

[15] Cavallini A, Boyer L, Luton M, Mirebeau P and Montanari G C 2015 Partial discharge testing of XLPE cables for HVDC: challenges and opportunities *Proc. 9th Int. Conf. Insulated Power Cables (Jicable'15)* Versailles

[16] Seltzer-Grant M, Giussani R, Siew W H, Corr E, Hu X, Zhu M, Judd M, Reid A, Neumann A and Awodola J 2015 Laboratory and field partial discharge measurement in HVDC power cables *Proc. 9th Int. Conf. Insulated Power Cables (Jicable'15)* Versailles

[17] Reid A, Seltzer-Grant M, Giussani R, Siew W H, Corr E, Zhu M, Hu X, Judd M and Mountassir O El 2015 Investigating the effects of VSC harmonic content on PD diagnostics for HVDC insulation systems *EPRI HVDC & FACTS Conf.* Palo Alto

[18] Judd M, Siew W H, Hu X, Corr E, Zhu M, Reid A, Mountassir O El, Urizarbarrena Cristobal M, Giussani R and Seltzer-Grant M 2015 Partial discharges under HVDC conditions *Euro TechCon* Warwickshire

[19] Corr E, Reid A, Hu X, Siew W H, Zhu M, Judd M, Seltzer-Grant M and Giussani R 2018 Partial discharge testing of defects in dielectric insulation under DC and voltage ripple conditions *CIGRE Sci. & Eng.* **N°11** 117-125

[20] Küchler A 2018 *High Voltage Engineering: Fundamentals - Technology - Applications* (Schweinfurt: Springer)

[21] Densley J 2001 Ageing mechanisms and diagnostics for power cables - an overview *IEEE Elect. Insul. Mag.* **17** 14-22

[22] IEC TC 42 2015 *IEC 60270:2000/AMD1:2015 Amendment 1 - High-voltage test techniques - Partial discharge measurements* (Geneva: IEC)
[23] ALSTOM Grid 2010 *HVDC for Beginners and Beyond* 2165-V2-EN
[24] Cigre WG D1.33 2010 *TB 444 - Guidelines for unconventional Partial Discharge measurements* (Paris: CIGRE)
[25] Mugala G, Eriksson R and Pettersson P 2007 Dependence of XLPE insulated power cable wave propagation characteristics on design parameters *IEEE Trans. Dielectr. Elect. Insul.* **14** 393-399
[26] Guo J J, Zhang L, Xu C and Boggs S A 2008 High Frequency Attenuation in Transmission Class Solid Dielectric Cable *IEEE Trans. Power Del.* **23** 1713-1719
[27] Papazyan R and Eriksson R 2003 Calibration for time domain propagation constant measurements on power cables *IEEE Trans. Instrum. Meas.* **52** 415-418
[28] Lemke E, Strehl T, Weissenberg W and Herron J 2006 Practical experiences in on-site PD diagnosis tests of HV power cable accessories in service *IEEE Int. Symp. Elect. Insul.* Toronto 498-501
[29] Reid A J, Judd M D, Stewart B G and Fouracre R A 2006 Partial discharge current pulses in SF6 and the effect of superposition of their radiometric measurement *J. Phys. D: Appl. Phys.* **39** 4167-4177
[30] Mazzanti G 2019 Activities of the DEIS technical committee on HVDC cable systems (cables, joints, and terminations) *IEEE Elect. Insul. Mag.* **35** 59-61
[31] Cigre WG B1.32 2012 *TB 496 - Recommendations for testing DC extruded cable systems for power transmission at a rated voltage up to 500 kV* (Paris: CIGRE)
[32] Tzimas A, Lucas G, Dyke K J, Perrot F, Boyer L, Mirebeau P, Dodd S, Castellon J and Notingher P 2015 Space charge evolution in XLPE HVDC cable with thermal-step-method and pulse-electro-acoustic *Proc. 9th Int. Conf. Insulated Power Cables (Jicable'15)* Versailles